THERMAL MODELLING OF LASER ABLATION SIMULATION BY NUMERICAL SOLUTION OF A THREE PHASE STEPHAN PROBLEM

G. Parissenti*, A. Niro**

* Politecnico di Milano, Energy Dept., Campus Bovisa, 20158 Milan - Italy, E-mail: guido.parissenti@mail.polimi.it
** Politecnico di Milano, Energy Dept., Campus Bovisa, 20158 Milan - Italy, E-mail: alfonso.niro@polimi.it

ABSTRACT

Laser ablation is an important industrial process to remove material from a solid surface by means of a laser beam that heats and evaporates or sublimates the material. One of the most interesting applications of such technique is the laser machining, technique that allow to drill holes and perform other operations on even very hard material in an extremely precise way. Usually this process is performed not continuously but with a pulsed laser, meaning that an extremely high amount of energy is discharged on an extremely small surface, achieving a strong energy density in a small amount of time such that the surrounding material absorbs a very small amount of energy; consequently it does not heat, preserving its properties. This process can be easily modeled as a three phase Stephan problem to which a finite difference solution with the Front Tracking Method is applied. Such methodology has been already used by authors to model electrodes erosion by the establishing of electric arches, with good agreement with literature data. The same methodology is now applied to laser ablation technique taking into account the additional energy contribution mechanisms that could have been previously negligible for an electric arc shock but that are of high relevance in a laser ablation process.

INTRODUCTION

The physical understanding of the laser ablation process involves many different phenomena such as energy absorption by electrons, energy transfer to lattice, heat conduction, phase transitions, ejection of droplets, ionization and plasma formation, and many others, being some of them more or less negligible depending on the laser intensity and the pulse duration. In femtosecond pulses it is not possible to consider the energy transfer from electrons to lattice by collision an instantaneous process [1], while in nanosecond pulses the dynamics of the phenomenon can be largely described by the conduction equation [2]. Nanosecond laser ablation represents a very interesting field of research due to its application in industry and in particular in material transformation. Mathematical models able to describe this process have continuously been proposed [3] but have always been extremely specific. Following this need, in this paper a Stefan multiphase thermal model of the laser ablation process is presented.
Historically, for this kind of problem very few analytical solutions have been found and only for the simplest cases with no more than two phases [4][5], applied for infinite or semi-infinite regions. The same solution can instead be easily obtained numerically [6] with the possibility of solving more difficult problems [7]. Three phase problems have been already solved numerically in the past [8] but using complex and low flexible finite-element methods, unsuitable to be inserted into larger codes for the simulation of complex physical problems involving not exclusively thermal phenomena. The authors proposed instead a different methodology, developing a numerical code which applies a common finite difference technique coupled with the Front Tracking Method.
This approach has already been successfully applied by the authors to the problem of high energy spot formation due to the onset of an electric arc [9], finding good agreement with experimental data. The purpose of this paper is hence the application of this general purpose multiphase solver code to the problem of nanosecond laser ablation. We will show the flexibility of the formulation as well as that the results obtained are in good agreement with the literature, taking into account where possible the additional contributions due to characteristics phenomena such as radiation and 1-dimensional mass release cooling. For this reason, following an approach suggested by literature, we do not consider fluences higher than 30 J/cm^2 because in this range effects not taken into account in our model, such as radial ejected mass and plasma expansion, are probably more significant [3].

PHYSICAL DESCRIPTION OF THE THERMAL MODEL

The spot created on a metal surface by a single laser pulse is usually performed on a surface much larger than its diameter, and at the same time it has usually a depth much smaller than its radius even at high fluences [10]. Taking into consideration the thermal dynamics, from an analytical point of view Lehr et al. [11] show that if the diffusion length $(\alpha_s t_d)^{1/2}$ is four times smaller than the metal target thickness by the incident heat flux direction, the metal plate itself can be considered infinite in extent (t_d is a phenomenon characteristic time like the total pulse time, e.g. 60 ns). For copper, as an example, this leads to a diffusion length of only 2.6 μm. Therefore, the problem can be considered as one-dimensional. A schematic representation of the model is sketched in Figure 1.
The model can be described as a semi-infinite solid (approximate as a slab of length $a \gg (\alpha_s t_d)^{1/2}$) in the region $X > 0$, where X is the spatial coordinate perpendicular to the surface, where the heat flux $F(t)$ is applied at $X = 0$. The $F(t)$ flux first

raises the solid temperature to the melting value T_m (Stage 1). At this time t_1 a new phase appears with a new domain for the liquid phase. Hence, the original slab is split into two different time-varying domains. While the surface S_1 moving following Eq. (3), the temperature in the liquid phase starts rising until the vaporization temperature T_v is attained at $t = t_2$ (Stage 2). At this time, the surface S_2 appears and starts moving following a relation similar to those for S_1(Stage 3).

We assume all thermal properties of the electrode are constant. Although in the vapor phase a temperature profile does not exist because vapor is assumed to be removed as soon as it forms, in the solid and liquid phases the temperature dynamic is ruled by the heat diffusion equations. At each moving surface, the Stefan Equation (described by Eq. 3,4) is introduced, to take into account the energy balance between the heat flux coming from the two phases and the change in internal energy due to the melting or vaporization. For the numerical solution, obviously, it is not possible to consider a semi-infinite domain, so we consider the solid as a slab in the domain $0 < X < a$ with $a \gg r$. Because of this hypothesis, we assume that at $X = a$ temperature should always remain equal to the initial temperature T_i , and temperature gradient is null. The verification of these conditions means that the region remains unchanged, whereas fixing one of these two boundary conditions at $X = a$ in the finite element code is only a matter of choice as both should be verified after the simulation. At this point the mathematical model can be described as follows.

Heat Diffusion Equations

$$k_s \frac{\partial^2 T_s}{\partial X^2} = \rho c_s \frac{\partial T_s}{\partial t} \text{ for } S_1 < X < a \quad (1)$$

$$k_l \frac{\partial^2 T_l}{\partial X^2} = \rho c_l \frac{\partial T_l}{\partial t} \text{ for } S_2 < X < S_1 \quad (2)$$

Stefan Equations on moving surfaces

$$k_s \frac{\partial T_s}{\partial X} - k_l \frac{\partial T_l}{\partial X} = \rho C_m \frac{dS_1}{dt} \text{ for } X = S_1, t > t_1 \quad (3)$$

$$k_l \frac{\partial T_l}{\partial X} - F(t) = \rho C_v \frac{dS_2}{dt} \text{ for } X = S_2, t > t_2 \quad (4)$$

Boundary conditions

$$T_s = T_i \text{ for } X = a \quad (5)$$

$$-k_s \frac{\partial T_s}{\partial X} = F(t) \text{ for } X = 0, t < t_1 \quad (6)$$

$$-k_l \frac{\partial T_l}{\partial X} = F(t) \text{ for } X = 0, t_1 < t < t_2 \quad (7)$$

$$T_s = T_l = T_m \text{ for } X = S_1 \quad (8)$$

$$T_l = T_v \text{ for } X = S_2 \quad (9)$$

Initial conditions

$$T_s = T_i \text{ for } t = 0 \quad (10)$$

$$S_1 = 0 \text{ for } t < t_1 \quad (11)$$

$$S_2 = 0 \text{ for } t < t_2 \quad (12)$$

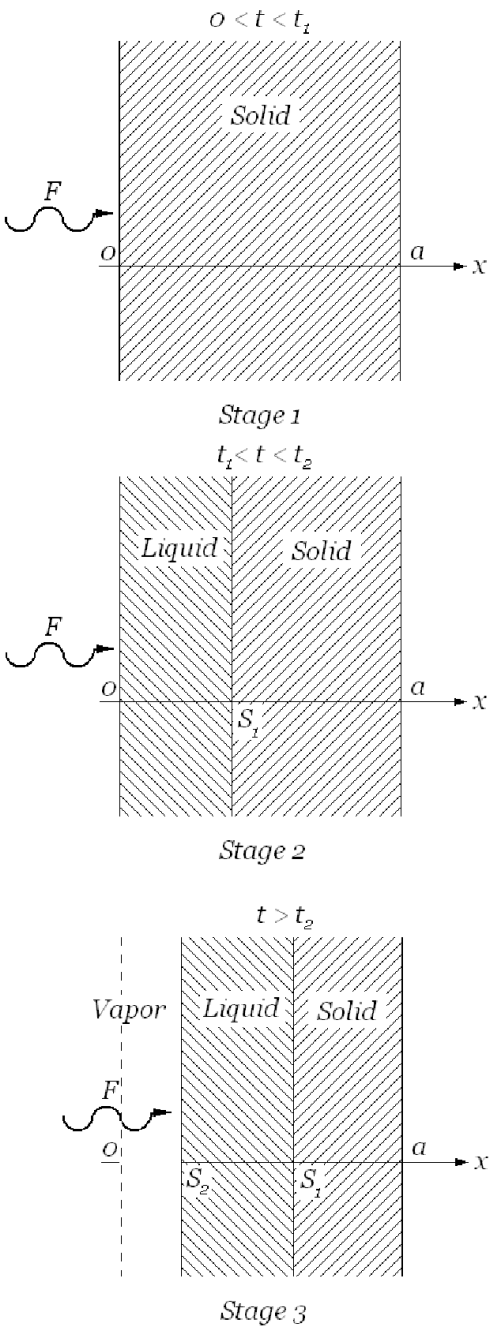

Figure 1. Stages of the model

Liquid and solid are considered to have the same density ρ to allow a simpler manipulation of the Stefan equations and to avoid thermal expansion. The error is no larger than around 10% for copper.

FINITE DIFFERENCES DISCRETIZATION AND FRONT TRACKING METHOD

The most difficult issue in using a finite difference method for this kind of problem is the time-dependance of the domains. We cannot assume the moving boundaries always lie on a node of the mesh, and therefore we do not have a unique domain. Considering two separate domains with different discretizations is also difficult, because at the beginning of the simulation one of them will be very small or null. To overcome these

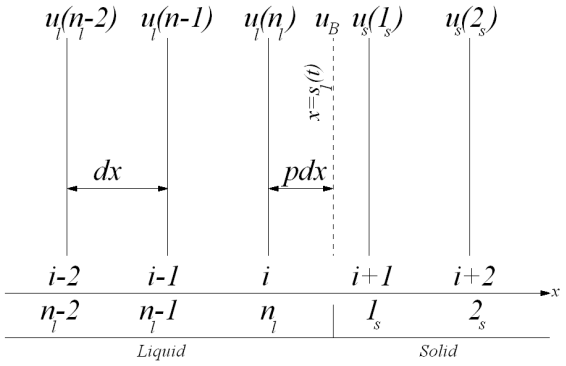

Figure 2. Lagrangian type interpolation for solid-liquid boundary

problems it is possible to use the Front Tracking method [5]. The positions S_1 and S_2 of the moving boundaries are obtained from the integration of the Stefan equations (3) and (4), and therefore they are not required to be a multiple of the mesh size. Let us say that at any time $k\delta t$ the phase-change boundary is located between two consecutive grid points, for example $i\delta X$ and $(i+1)\delta X$. In order to define the finite difference form of the heat diffusion equations (1) and (2) for these two points, we need to use a second order Lagrangian interpolation that allows unequal spatial intervals. We will see that the appearance of the solid-liquid boundary requires us to lower to one the order of the interpolation for the initial step because the domain is restricted to only one node.

LAGRANGIAN TYPE INTERPOLATION - The Lagrangian type interpolation method used by Crank [5] allows a modification of the finite difference formulae incorporating unequal spatial intervals near the moving boundary. Using a 2^{nd} order scheme based on three points, a generic function $u(x)$ can be represented as

$$u(x) = \sum_{j=0}^{2} l_j(x) u(a_j) \tag{13}$$

$$l_j(x) = \frac{p_2(x)}{(x-a_j)\left.\frac{dp_2(x)}{dx}\right|_{x=a_j}} \tag{14}$$

$$p_2(x) = (x-a_0)(x-a_1)(x-a_2) \tag{15}$$

where $u(a_0), u(a_1), u(a_2)$ are three known values of $u(x)$ at the points $x = a_0, a_1, a_2$ respectively. From $u(x)$, it is possible to obtain the 1^{st} and 2^{nd} derivatives expressed in terms of a_j.

Referring to Figure 2, the moving boundary between liquid and solid is shown to be located at a fractional distance pdx from the considered node i, and hence it is possible to specialize the above formulas to obtain the derivative in these two spatial intervals. Substituting the following values for a_j and $u(a_j)$, pertaining to the solid phase

$\mathbf{a_j}$	$\mathbf{u(a_j)}$
$a_0 = (i+1-(1-p))\,dx = (i+p)dx$	u_B
$a_1 = (i+1)dx$	$u_s^{i+1} = u_s^1$
$a_2 = (i+2)dx$	$u_s^{i+2} = u_s^2$

we can write $s_1(kd\tau) = (i+p^k)dx$. Starting from equation (3), applying a non-dimensionalization with characteristic parameters, and using the first-order Euler approximation of ds/dt we can obtain

$$p^{k+1} = p^k + \frac{d\tau}{dx}\left(\gamma_s \frac{\partial u_s}{\partial x} - \gamma_l \frac{\partial u_l}{\partial x}\right) \tag{16}$$

where γ_s and γ_l are nondimensional values depending on the physical characteristics of the material. Equation (16) is valid for the solid-liquid moving boundary in Stages 2 and 3. Analogously, a parameter v can be used to track the liquid-vapor moving boundary with a similar equation. To manage the movement of the boundaries, we update at every time step the fractional parameters p and v. Their values lie between 0 and 1, i.e., the relative boundary lies between two nodes, except for $p > 1$, which means that the moving boundary passed a node. To simulate this, we remove the node from the solid domain and add a node to the liquid one. Calculating $p^{k+1} = p^k - 1$, we obtain the starting p for the spatial interval dx. For the liquid-vapor boundary, we simply remove one node from the liquid domain without any additional operation, following the assumption the vapor is continuously removed from the surface.

CODE APPLICATION

The numerical code has been modified in order to take into account typical laser ablation phenomena. The most easy to implement is thermal radiation, able to remove a small portion of the provided power input from the surface. It is easily implemented building $F(t)$ of Eqs. (4),(6) and (7) in the following way:

$$F(t) = \tilde{F}(t) - q_r(t) \quad \text{where} \quad q_r(t) = \sigma\varepsilon\left(T_{surf}^4 - T_i^4\right)$$

A second important contribution is the effects of the released mass that implies two important phenomena. The ejected mass flux can be defined as:

$$\dot{m}(t) = \frac{dS_2}{dt} A_s \rho \tag{17}$$

The first effect that such mass flow rate produces is the surface cooling, because the vapor mass leaves the laser spot with a kinetic energy that lowers the laser power input. The second effect is a sort of shielding produced by this vapor mass in front of the surface: the highest part of the laser energy is absorbed to ionize the vapor creating a plasma that is even additionally heated. The amount absorbed by the plasma do not reach the surface, lowering the effective fluence and so the total ablation depth. In nanosecond laser pulses this plasma effect is not negligible even at low fluences [12].
From the mathematical point of view it is not possible to calculate the amount of ejected mass and then later calculate the energy transported away by the boundary. In fact in some situations, such as a decrease in the incoming heat flux, this value can be bigger than the heat flux itself, realizing a non physical situation. We need to consider this contribution as occurring simultaneously with the mass ejection, and in doing so Eq. (4) is modified in the following way:

$$k_l \frac{\partial T_l}{\partial X} + F(t) - n v_{th} \frac{3}{2} k_B T_v = \rho C_v \frac{dS_2}{dt} \tag{18}$$

The added term is an outbound energy flux subtracted to the incoming $F(t)$ given by the kinetic energy of the atoms that leave the surface at a speed equal to the random thermal velocity v_{th}. A Maxwellian kinetic energy distribution is assumed. n is the neutral atoms number density defined as:

$$n = \frac{\dot{m}(t)}{M_a A_s v_{th}} \tag{19}$$

If we substitute Eqs. (17) and (19) into Eq. (18) we obtain:

$$k_l \frac{\partial T_l}{\partial X} + F(t) - \frac{dS_2}{dt} \frac{\rho}{M_a} \frac{3}{2} k_B T_v = \rho C_v \frac{dS_2}{dt} \tag{20}$$

hence we arrive to the final form

$$k_l \frac{\partial T_l}{\partial X} + F = \rho \bar{C_v} \frac{dS_2}{dt} \tag{21}$$

where $\bar{C_v}$ is a modified latent heat of vaporization that takes into account the contribution of the cooling term

$$\bar{C_v} = C_v + \frac{3}{2} \frac{k_B T_v}{M_a} \tag{22}$$

We can notice that the same result has been obtained by Beilis [13] in writing the anode energy balance for a graphite anode spot model.
This elaboration takes into account only the first effect of the mass ejection, the cooling effect. In order to take into account the laser absorbed energy by the ejected mass, Eq. (22) has been modified in the following way:

$$\bar{C_v} = C_v + \Lambda \frac{3}{2} \frac{k_B T_v}{M_a} \tag{23}$$

if $\Lambda = 1$ only the cooling effect is taken into account, otherwise this parameter allows to introduce an heat flux loss from the surface proportional to the ejected mass flow rate. This simplification of the problem physics, that allows to avoid the introduction of an ionization model and balance equations of plasma mass and momentum, is based on the assumption that the reduction of the heat flux due to the vaporized material absorption is linearly proportional to the ejected mass flow rate. Following this approach it is possible to tune the Λ parameter in order to fit experimental data and observe if varying the initial condition of laser fluence the code is able to correctly follow the trend of experimental data.

Our code has been applied to the work of Zeng et al. [14], where a nanosecond 355 nm Nd:YAG laser pulse of 60 ns FWHM with various fluences has been directed on a copper target. Zeng were able to find a linear relation between the applied fluence and the ablation rate per pulse. The Λ parameter has been set to two values in order to produce results in accordance with the line interpolating the experimental data at 6 $J/cm^2 (\Lambda = 34.5)$ and 18 $J/cm^2 (\Lambda = 41.6)$ of fluence. Then multiple simulations has been carried out with those fixed Λ at 6, 10, 15 and 18 J/cm^2. The original data from Zeng and the result obtained with our code are shown in Figure 3.

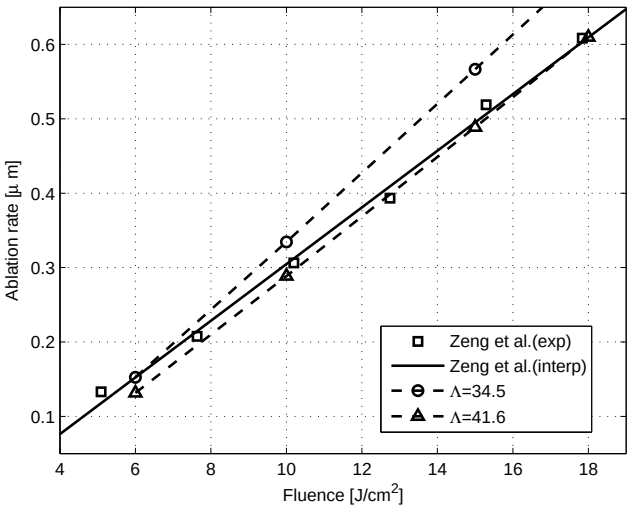

Figure 3. Zeng and authors' code results

It can be clearly seen that in accordance with the experiment the code shows a linear dependency of solution from the introduced energy as reported by Zeng. The slope of the solution is different instead, depending on the value of Λ, which increases from low fluences to relatively high fluences, meaning that an higher amount of laser energy is shielded by the ejected material, and only a small part of the emitted fluence actually arrives on the surface. This result is in accordance with the observation of Zeng even if only from a qualitative point of view.

From simulations it is possible to quantify the plasma shielding losses. In Figure 4 and Figure 5 we plotted for the two

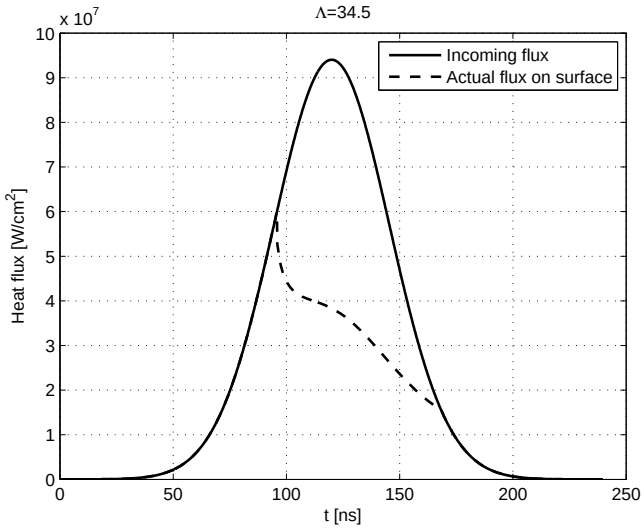

Figure 4. Heat fluxes provided and absorbed at $\Lambda = 34.5$ and fluence of 6 J/cm^2

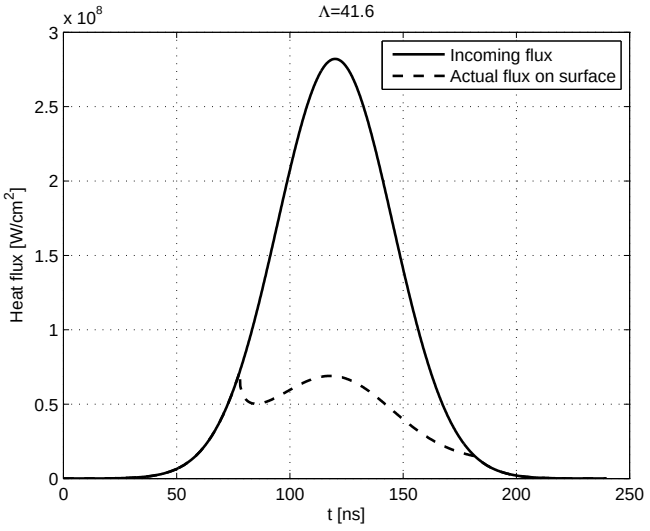

Figure 5. Heat fluxes provided and absorbed at $\Lambda = 41.6$ and fluence of 18 J/cm^2

previously mentioned conditions the provided energy flux and the flux that actually reach the surface after the shielding.

Even graphically it is possible to see that with fluence of 6 J/cm^2, to be compatible with experimental data, the ratio between the provided energy and the energy that actually reaches the surface is less than the case with fluence of 18 J/cm^2 shown in Figure 5. Integrating the effective flux we obtain in the first case an effective fluence of 3.5 J/cm^2 that means a ratio of 1.7 between provided and absorbed flux. In the second case this ratio is equal to 3, meaning that only 6 J/cm^2 are able to reach the metal surface. Such values are compatible from those provided by Gojani et al. [2] which observe that using a self-regulating plasma model the ratio between the energy delivered and the energy spent into evaporation is 2.3, even if related to higher order of magnitude of fluence.

It is interesting to point out that, as expressed by Eqs. (20) and (21), the Λ parameter is the multiplier of a term that is proportional to dS_2/dt or to the velocity of the ablated surface. Even if we previously calculate this value only taking into account the metal evaporation this does not mean that the value of Λ, set in order to fit the experimental data, does not take into account other causes of the movement of the boundary. In other words another very important phenomenon in laser ablation, represented by the ejection of droplets due to the explosion of the surface caused by high fluences, could still be taken into consideration with the approach proposed in this paper. Again, this because Λ takes into account the shielding of the laser beam due to a mass of material proportional only to the ablation rate. Adjusting the parameter in order to fit the experiment means to take into account also other sources of ablation other than evaporation.

CONCLUSIONS

The numerical solution of a one dimensional, three-phases Stefan problem has been applied to the a problem of nanosecond laser ablation. The fundamental equations governing the phenomenon and the numerical approach used to solve the problem has been described. This multipurpose code has been modified with a suitable parameter able to take into account the laser energy absorbed by the ablation created plasma in order to fit with experimental data. Results are in agreement with the general understanding of the phenomenon which foresee and higher plasma shielding for higher fluences, and the use of the before mentioned parameter allows to quantify such shielding assuming that the ablation is mainly driven by the thermal dynamic of the metal. The quantification of the plasma shielding is in accordance with values reported by other authors.

NOMENCLATURE

a	Slab length (m)
c	Specific heat (J/kgK)
C	Latent heat (J/kg)
$F(t)$	Inbound heat flux (W/m^2)
k	Thermal conductivity (W/mK)
K_B	Boltzmann constant (kg/s^2K)
M_a	Atom mass (kg)
n	Neutral atoms number density ($1/m^3$)
p	Fractional parameter for the s_1 tracking
q_b	Heat flux (assumed constant) (W/m^2)
S	Interface dimensional position (m)
s	Interface non-dimensional position
t	Time (s)
T_i	Initial system temperature (K)
T	Temperature (K)
u	Non-dimensional temperature
v	Fractional parameter for the s_2 tracking
v_{th}	Thermal velocity (m/s)
X	Dimensional spatial coordinate (m)
x	Non-dimensional spatial coordinate
Λ	Fitting parameter ($-$)
ρ	Density (kg/m^3)
τ	Non-dimensional time

Subscripts

l	Liquid
m	Melting
s	Solid
v	Vapor
1	Solid-Liquid
2	Liquid-Vapor

REFERENCES

[1] B. N. Chichkov, C. Momma, S. Nolte, F. von Alvensleben, and A. Tunnermann. Femtosecond, picosecond and nanosecond laser ablation of solids. *Appl. Phys. A: Materials Science & Processing*, 63(2):109–115, Jul 1997.

[2] Ardian B. Gojani, Jack J. Yoh, and Jong H. Yoo. Extended measurement of crater depths for aluminum and copper at high irradiances by nanosecond visible laser pulses. *Applied Surface Science*, 255(5, Part 2):2777 – 2781, 2008.

[3] S. Laville, F. Vidal, T. W. Johnston, O. Barthélemy, M. Chaker, B. Le Drogoff, J. Margot, and M. Sabsabi. Fluid modeling of the laser ablation depth as a function of the pulse duration for conductors. *Phys. Rev. E*, 66(6):066415, Dec 2002.

[4] H. S. Carslaw and J. C. Jaeger. *Conduction of heat in solids*. Oxford University Press, 2^{nd} edition edition, 1959.

[5] J. Crank. *Free and moving boundary problems*. Oxford University Press, 1984.

[6] A. Kharab. Spreadsheet simulation of the moving bound-

ary of the one-phase stefan problem. *Comput. Methods Appl. Mech. Engrg.*, 145:217–225, 1997.

[7] D. R. Atthey. A finite difference scheme for melting problems. *J. Ins. Maths Applics*, 13:353–366, 1974.

[8] R. Bonnerot and P. Jamet. A conservative finite element method for one dimensional stefan problems with appearing and disappearing phases. *J. Comput. Phys.*, 41:357–388, 1981.

[9] G. Parissenti and A. Niro. Finite differences solution of a three-phase stefan problem with high power input. *Proceedings of the XXVII UIT Congress, Reggio Emilia (Italy)*, 22-24 June 2009.

[10] J. P. Colombier, P. Combis, F. Bonneau, R. Le Harzic, and E. Audouard. Hydrodynamic simulations of metal ablation by femtosecond laser irradiation. *Phys. Rev. B*, 71(16):165406, Apr 2005.

[11] F. M. Lehr and M. Kristiansen. Electrode erosion from high current moving arcs. *IEEE Trans. Plasma Sci.*, 17(5):811–817, 1989.

[12] S. Amoruso, M. Armenante, V. Berardi, R. Bruzzese, and N. Spinelli. Hydrodynamic simulations of metal ablation by femtosecond laser irradiation. *Appl. Phys. A: Materials Science & Processing*, 65(3):265–271, Sept 1997.

[13] I.I. Beilis. Anode spot vacuum arc model: graphite anode. *IEEE T. Compon. Pack. T.*, 23(2):334–240, June 2000.

[14] D. W. Zeng, K. C. Yung, and C. S. Xie. Uv nd:yag laser ablation of copper: chemical states in both crater and halo studied by xps. *Applied Surface Science*, 217(1-4):170 – 180, 2003.